CHEMISTRY OF MATERIALS
Article

Chem. Mater. **2010,** *22,* 3909–3915 3909
DOI:10.1021/cm1001016

Flexible, Adhesive, and Biocompatible Bragg Mirrors Based on Polydimethylsiloxane Infiltrated Nanoparticle Multilayers

Mauricio E. Calvo and Hernán Míguez*

Instituto de Ciencia de Materiales de Sevilla, Consejo Superior de Investigaciones Científicas, Universidad de Sevilla, Spain

Received January 12, 2010. Revised Manuscript Received May 31, 2010

Herein we present a series of self-standing, flexible, and biocompatible optical interference filters obtained through infiltration and polymerization of an elastomer (polydimethylsiloxane) in a porous Bragg mirror prepared by alternating deposition of layers of TiO_2 and SiO_2 nanoparticles. The method proposed yields the uniform filling of the nanopores of the multilayer by the polymer, which allows lifting off the hybrid structure as long as the ensemble is cooled to temperatures below the glass transition of the polymer. This multifunctional material combines the optical properties of the periodic nanoporous multilayer and the structural and physicochemical characteristics of polydimethylsiloxane. Experimental demonstrations of their potential use as flexible and adhesive UV-protecting filters, as well as of light, highly-efficient conformal back reflectors to enhance the efficiency of photovoltaic devices are provided.

Introduction

Optical interference filters based in periodic multilayer systems are well-known and highly developed passive optical devices.[1] Such structures, also known as distributed Bragg reflectors, acquire their optical properties through the periodic modulation of the refractive index, so they are also classified as one-dimensional photonic crystals (1DPC). Many applications of these materials can be found in all branches of optics as precise frequency selective filters or as antireflective coatings. Although most routes of fabrication of such multilayer structures are based on physical deposition, some successful methods have been developed within the field of materials chemistry.[2] Within this approach, two transparent metal oxides, namely SiO_2 and TiO_2, are the most used compounds since they present very different dielectric constant ($n_{SiO_2} = 1.45$; $n_{TiO_2} = 2.44$) and can be deposited easily from a liquid phase by either spin or dip coating.[3,4] Since the deposits can be shaped as thin films, 1DPC can be used to protect surfaces against radiation or, in a recent application, integrated in solar cells to enhance conversion efficiencies.[5] However, it is very difficult to find, either in the market or in the technical or scientific literature, interferometric mirror films adaptable to all kinds of surfaces, including human skin. This limitation lies basically in the mechanical properties of both the substrates and the materials employed for the preparation of most interference filters developed up to date, which results in highly rigid coatings not suitable to be adapted to surfaces of arbitrary curvature or different physico-chemical properties.

Previous successful efforts to obtain flexible 1DPC were based on the lamellar self-assembly of a mixture of polymers.[6] In this case, the refractive index contrast between layers is low and it is necessary to stack a high number of layers (on the order of hundreds) in order to achieve a significant reflectance (above 70%). On the other hand, polymers can be incorporated as one of the building layer (constituting the low R.I. layer) in these periodic structures[7] or as a medium to disperse oxide particles.[8,9] All structures obtained in these works behave as highly efficient reflectors (reflectance close to 100%) in the IR part of the electromagnetic spectrum, as a result of the large thickness of the individual constituent layers in the Bragg mirror. In addition, the synthetic procedures required involve the use of nonenvironmentally friendly and expensive solvents, precursors, or monomers. In most cases, a previous surface treatment is necessary to obtain good uniformity and adherence of the following deposited layers.[10] In the related field of self-assembled three-dimensional

*Corresponding author. Address: Américo Vespucio 49, 41092 Sevilla, Spain. Ph +34 954 48 95 81. Fax +34 954 46 06 65. E-mail: hernan@icmse.csic.es.

(1) Macleod, H. A. *Thin Film Optical Filters*, 3rd ed.; Institute of Physics Publishing: London, 2001.
(2) Hinczewski, D. S.; Hinczewski, M.; Tepehan, F. Z.; Tepehan, G. G. *Sol. Energy Mater. Sol. Cells* **2005**, *87*, 181.
(3) Almeida, R. M.; Rodrigues, A. S. *J. Non-Cryst. Solids* **2003**, *326*, 405.
(4) Rabaste, S.; Bellessa, J.; Brioude, A.; Bovier, C.; Plenet, J. C.; Brenier, R.; Marty, O.; Mugnier, J.; Dumas, J. *Thin Solid Films* **2002**, *416*, 242.
(5) Colodrero, S.; Mihi, A.; Häggman, L.; Ocaña, M.; Boschloo, G.; Hagfeldt, A.; Míguez, H. *Adv. Mater.* **2009**, *21*, 764.
(6) Urbas, A.; Sharp, R.; Fink, Y.; Thomas, E. L.; Xenidou, M.; Fetters, L. J. *Adv. Mater.* **2000**, *12*, 812.
(7) DeCorby, R. G.; Ponnampalam, N.; Nguyen, H. T.; Clement, T. J. *Adv. Mater.* **2007**, *19*, 193.
(8) Druffel, T.; Mandzy, N.; Sunkara, M.; Grulke, E. *Small* **2008**, *4*, 459.
(9) Mennig, M.; Oliveira, P. W.; Frantzen, A.; Schmidt, H. *Thin Solid Films* **1999**, *351*, 225.
(10) Girshevitz, O.; Nitzan, Y.; Sukenik, C. N. *Chem. Mater.* **2008**, *20*, 1390.

Published on Web 06/14/2010

photonic crystals, flexible films displaying structural color have been attained,[11] although the small dielectric contrast and the presence of intrinsic defects results in too low reflectance as to consider them efficient radiation protective coatings.

Recently, a new series of 1DPC were developed alternating layers of different nanoparticulated oxides to obtain porous Bragg mirrors.[12−14] In this kind of structures the porosity plays an important role in determining the refractive index of each layer and thus the dielectric contrast existing between them. The versatility of the approach has been proven by preparing periodic stacks of films made of SiO_2, TiO_2, or SnO_2 nanoparticles. Also, it is possible to make a porous 1DPC using only TiO_2 nanoparticles with different aggregation states conferring photoconducting properties to the ensemble.[15] As these structures are porous, they can be infiltrated with small testing molecules in vapor or liquid phase, causing a modification of the optical properties.[16]

We recently demonstrated that porous Bragg mirror structures can be infiltrated with polymers, constituting the first example of a hybrid polymer−nanoparticle 1DPC.[17] In that case, we used a methylene chloride solution of poly(bis-phenol A)carbonate to obtain a hybrid inorganic−polymeric film that can be peeled from the substrate to make a flexible and transferable highly reflecting 1DPC. Applications of this new kind of flexible 1DPC are restricted only by the viscoelastic properties of the polymer whose glass-transition temperature (T_g) is near 420 K,[18] which limits the flexibility of the ensemble, and by the lack of full biocompatibility of polycarbonate.

In this work, we present a novel series of hybrid 1DPCs built by integration of TiO_2 and SiO_2 nanoparticle multilayer in a polydimethylsiloxane (PDMS) film, a fully biocompatible and environmental friendly polymer. PDMS is chemically inert, thermally stable, permeable to gases, simple to handle and manipulate, and exhibits isotropic and homogeneous properties.[19] The synthetic procedure is based on the infiltration of the mesopores of the multilayer with a mixture of oligomers and a polymerizing agent. Such an approach yields higher filling fractions of the infiltrated polymer than those obtained by the solution method previously developed by us, and allows us to easily lifting the polymerized deposited off the substrate they are originally deposited onto. The robustness and flexibility of the final free-standing optical interference filters are largely enhanced by the use of PDMS. Remarkably, the optical quality of the self-supported Bragg mirrors is similar to that observed for the same deposits before lifting them off the substrate. The mechanical stability of the final ensemble is a direct consequence of the low T_g of PDMS, which makes it highly flexible at room temperature. In addition, PDMS is biocompatible and stable in biological media[20,21] with a probed capability to be integrated in biosensors.[22] All these features are maintained in these hybrid 1DPCs that, may be employed as efficient shields against any undesirable radiation, including the harmful ultraviolet A (UVA) range. Because the reflected color has a structural origin, protection is achieved without involving photon absorption and the consequent heating or activation of chemical species. Additionally, as polymerization was realized in situ, we can modify the adhesive properties of PDMS in order to reversibly coat these mirrors with any kind of surfaces (including human skin) or to easily attach them to solar cells where they behave as mirrors capable of reflecting nonabsorbed photons back into the cell, increasing the device efficiency.

Experimental Section

Preparation of Particulate Suspensions. TiO_2 nanoparticulated sols were synthesized using a procedure based on the hydrolysis of titanium tetraisopropoxide ($Ti(OCH_2CH_2CH_3)_4$, 97%, Aldrich) as has been described before. Briefly, titanium tetraisopropoxide was added to Milli-Q water. The white precipitate was filtered and washed several times with distilled water. The resultant solid was peptized in an oven at 120 °C for 3 h with tetramethylammonium hydroxide (Fluka). Finally, the suspension obtained was centrifuged at 14.000 rpm (rpm) for 10 min. SiO_2 nanocolloids were purchased from Dupont (LUDOX TMA, Aldrich). Both suspensions were diluted in methanol to a range from 2 to 4 wt % for TiO_2 and 2 to 4 wt % for SiO_2 particles.

Deposition of Nanoparticle-Based One-Dimensional Photonic Crystals. Photonic crystals were built by an alternated deposition of TiO_2 and SiO_2 nanoparticulated suspensions, following a generic procedure previously reported by our group.[13] These sols were deposited over glass slides using a spin coater (Laurell WS-400 $\times$ 10^{-6}NPP) in which both the acceleration ramp and the final rotation speed could be precisely determined. Final speed was chosen between nominal value of 4000 and 8000 rpm and accelerations were selected between nominal 4550 and 7150 rpm s^{-1}. The total spin-coating process (ramping-up and final speed) is completed in 60 s. Afterward, the coated sample is maintained at 25 °C during 5 min in a closed chamber. Sequentially, another layer of a different type of nanoparticle is deposited following the procedure described above. The process is repeated until all layers have been deposited.

Polymerization into the Mesopore Voids and Transferring. The usual procedure is to make a liquid dispersion with the elastomer precursor (EP) and the curing agent (CA) (Sylgard 184 elastomer kit, Dow Corning) . The mass ratio EP:CA of these

(11) Arsenault, A. C.; Clark, T. J.; von Freyman, G.; Cademartiri, L.; Sapienza, R.; Bertolotti, J.; Vekris, E.; Wong, S.; Kitaev, V.; Manners, I.; Wang, R. Z.; John, S.; Wiersma, D.; Ozin, G. A. *Nat. Mater.* **2006**, *5*, 179.
(12) Wu, Z.; Lee, D.; Rubner, M. F.; Cohen, R. E. *Small* **2007**, *3*, 1445.
(13) Colodrero, S.; Ocaña, M.; Miguez, H. *Langmuir* **2008**, *24*, 4430.
(14) Puzzo, D. P.; Bonifacio, L. D.; Oreopoulos, J.; Yip, C. M.; Manners, I.; Ozin, G. A. *J. Mater. Chem.* **2009**, *19*, 3500.
(15) Calvo, M. E.; Colodrero, S.; Rojas, T. C.; Ocaña, M.; Anta, J. A.; Míguez, H. *Adv. Funct. Mater.* **2008**, *18*, 2708.
(16) Colodrero, S.; Ocaña, M.; González-Elipe, A. R.; Míguez, H. *Langmuir* **2008**, *24*, 9135.
(17) Calvo, M. E.; Sánchez-Sobrado, O.; Lozano, G.; Míguez, H. *J. Mater. Chem.* **2009**, *19*, 3144.
(18) Plazek, D. J.; Ngai, K. L. *Physical Properties of Polymers Handbook*, 2nd ed.; Mark, J. E., Ed.; Springer Science and Business Media: Chicago, 2007; pp 211−212.
(19) Xia, Y. N.; Whitesides, G. M. *Angew. Chem., Int. Ed.* **1998**, *3*, 551.
(20) Lee, E. J.; Baek, D. H.; Baek, J. Y.; Kim, B. J.; Choi, J.; Pak, J. J.; Lee, S. H. *IEEE Sens. J.* **2009**, *6*, 625.
(21) Mata, A.; Fleischman, A. J.; Roy, S. *Biomed. Microdevices* **2005**, *4*, 281.
(22) Baek, J; An, J.; Choi, J.; Park, K.; Lee, S. *Sens. Actuators, A* **2008**, *143*, 423.

two compounds can vary from 2 to 0.5 to modify the adherence of the final product. Next, the infiltration of the dispersion can be made depositing a certain amount onto the multilayers using a roller blade or by spin coating (40 s, 1000 rpm). Thinner PDMS layers are obtained with this last method. After that, samples were cured at 120 °C in a stove during 30 min. Next, we made straight incisions in the PDMS layer with a blade, and we immersed the infiltrated multilayer supported onto the glass in liquid nitrogen (77K). We then allowed samples to get to room temperature, and at the same time, the films were lifted from the substrate.

Optical Characterization. Reflectance spectra were performed using a Fourier Transform infrared spectrophotometer (Bruker IFS-66 FTIR) attached to a microscope and operating in reflection mode with a 4X objective with 0.1 of numerical aperture (light cone angle ±5.7°). Transmittance spectra were acquired using a Perkin-Elmer UV−vis Lambda 12 spectrometer. Film images were acquired using a digital camera (Canon EOS 400D).

Structural Characterization. Field Emission Electron Microscopy (FESEM) images of the multilayers films deposited onto silicon were taken by using a microscope Hitachi 5200 operating at 5 kV. Cross section on the self-standing multilayers were obtained by cutting samples with a sharpen scalpel and applying silver paint from the edges of the sample to the microscope specimen support to minimize charge effects under the electron beam.

Dye Sensitized Solar Cells Photoelectrochemical Measurements. Fabrication and ensemble of the Dye Sensitized Solar Cells (DSSC) were reported elsewhere.[5] The photocurrent spectra were measured in the spectral range comprised between 400 and 800 nm. TiO_2 electrode was illuminated through transparent conductive oxide (TCO). Light originated in a 450 W xenon lamp (Oriel) was monochromated using alternatively a diffraction grating (400−800 nm, 1200 lines/mm, Oriel). Slits were chosen to attain 10 nm resolution and a 400 nm cut off filter was used. Currents were measured using an Autolab PGSTAT 128N. Flexible mirrors were stuck directly onto the external face of the counter electrode.

Results and Discussion

Microstructure. To build the porous one-dimensional photonic crystals we will use as matrices, it is necessary to employ suspensions of colloidal particles of nanometer-size. Photocorrelation spectroscopy results (Figure 1) show that both precursors contain particles with narrow size distribution. Analysis was carried out in the same media used to deposit the particles.The alternated deposition of these SiO_2 and TiO_2 nanocolloids by spin-coating from their respective precursor suspensions leads to a multilayered assembly of photonic crystal properties.[13] Microstructure of these porous 1DPC can be explored by FESEM. An image of the cross section of a SiO_2−TiO_2 nanoparticle stack reveals a well-defined layer thickness with smooth interfaces between them (Figure 2a). These two features make such structures suitable to generate a periodic modulation of the refractive index in one direction of the space as it was demonstrated in previous works. Once PDMS oligomers are deposited by either spin coating or Dr. Blade, pores are filled, as can be confirmed by observation of the cross-sections of the TiO_2 and SiO_2 layers at different magnifications under the FESEM (Figure 2b−d). Spherical particles are SiO_2 nanocolloids,

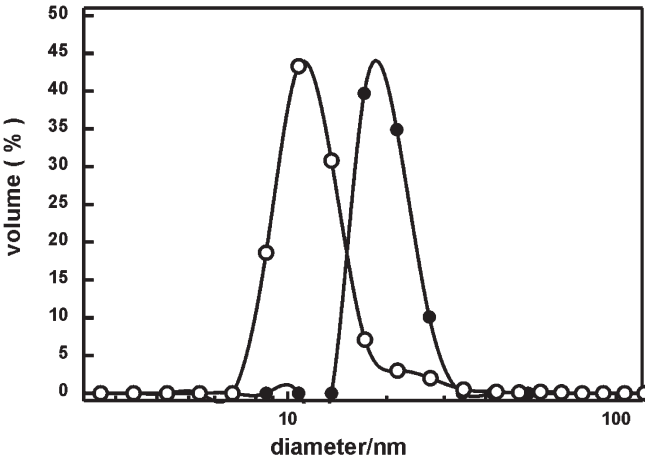

Figure 1. Particle size distribution (% volume) of the nanoparticulated suspensions of SiO_2 (black circles) and TiO_2 (white circles) used to build the multilayer structure.

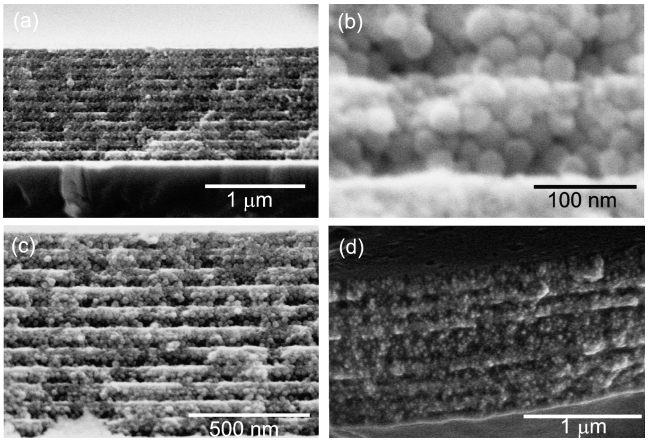

Figure 2. FESEM images of cross sections of different nanoparticle based 1DPCs: (a) a 20-layer-thick film deposited on a silicon wafer; (b) detailed image of the interface between SiO_2 and TiO_2 nanoparticle layers after being filled with PDMS; (c) the multilayer shown in image a after infiltration with PDMS; (d) PDMS infiltrated multilayer in which an optical defect has been controllably introduced in the middle of the stack.

whereas smaller and elongated particles are TiO_2 nanocrystallites. Both kinds of particles seem to have been uniformly covered by a polymeric compound (Figure 2b). Lower-magnification images reveal that the polymerization into the voids preserves the periodicity existing in the original multilayer (Figure 2c) without cracks or distortion of the interfaces. In Figure 2d, we show the cross-section of an infiltrated multilayer containing a disruption of the periodicity achieved by depositing a thicker layer of SiO_2 in the middle of the stack.

Please notice that the method developed may be considered a generic procedure to infiltrate polymers within nanometer size voids, which we believe is demonstrated in this manuscript for the first time. The first difference with previous works is that a mixture of oligomers and a catalyst were infilled in the voids, since it was not possible to dissolve and infiltrate the PDMS. Thus, polymerization takes place inside the porous matrix in this new approach. Second, in order to cleanly remove the hybrid ensemble from the substrate, we had to cool the structure down to the glass

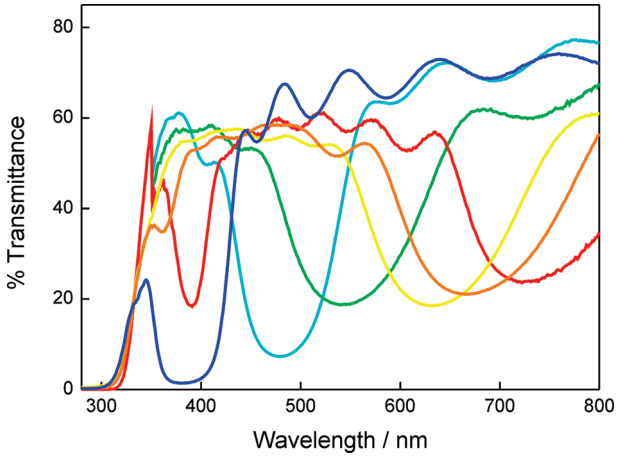

Figure 3. Transmittance spectra of self-standing hybrid PDMS-1DPC obtained employing different spin-coating conditions (final velocity between 4000 and 8000 rpm) and concentrations of TiO_2 suspension (2−4 wt %).

transition temperature of the polymer, which prevented the formation of a surface patterned PDMS film. By doing this, we avoid attaining a mere replica of the outer surface of the multilayer, and instead favor that the whole multilayer is strongly held by the polymer and peeled off the substrate. Please bear in mind that PDMS is the main polymeric compound used to perform soft-lithography. Thus, it conformally adapts to and replicates any surface it is deposited on, but its infiltration on nanometer-size voids in order to incorporate an inorganic structure in a polymeric film is not trivial and has never been achieved before.

Optical Properties of Supported and Self-Standing Optical Interference Filters. The existence of a periodic modulation of the refractive index in the direction perpendicular to the nanoparticle layers gives rise to optical interference effects that result in the opening of a forbidden photon frequency range along that direction. This feature is recognized as a maximum (or a minimum) in the reflectance (or transmittance) spectra. The spectral position of this peak can be changed by modifying the thickness of the layers, which can be easily made by varying the concentration of the nanocolloids in the precursor suspensions[13] or the spin coating operational parameters (final rotation speed and acceleration ramp).[23] In Figure 3 we show UV−visible transmittance spectra of twelve-layer flexible and self-standing 1DPCs processed by spin coating and used as hosts for PDMS infiltration. Two types of bands are distinguished. The one whose edge is at $\lambda = 340$ nm is an absorption band consequence of direct electronic transitions in the anatase nanoparticles. As expected, its spectral position remains unchanged as the structural parameters of the multilayer are varied, because the same TiO_2 colloids are used for all of them. The second band is blue-shifted as the thickness of the constituent layers decreases, which indicates that has a structural origin. The spectral position of this Bragg peak can be precisely tuned across the entire visible and UV regions. A clear trend is observed for the transmittance minimum intensity, which tends to decrease as we approach

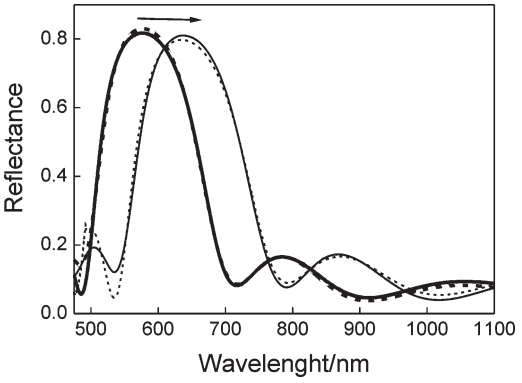

Figure 4. Specular reflectance spectra obtained from a 10-layer-nanoparticle-based 1DPC before and after infiltration of PDMS (solid lines). The arrow indicates the direction of the shift of the Bragg peak to higher wavelengths because of the infiltration of PDMS. Dashed lines correspond to the optimized fittings for each spectrum.

the UV region in spite of the fact that all multilayers present the same number of layers and similar refractive index contrast. A thorough and systematic comparison to simulated spectra allow us to confirm that such improvement of the blocking properties of the coating operating in the UV region is not due to higher structural quality, but just to the theoretically expected increase of the scattering strength[24] of the ensemble as the filling fraction (defined as the ratio between the thickness of a particular layer and the total thickness of the unit cell) of the TiO_2 layer is diminished. Theoretical curves exemplifying such effect are provided as Supporting Information. Thus, the transmittance minimum can reach values near 1% with planar spectral response in the UV region. This kind of response determines the potential use of these hybrid photonic crystals as flexible and free-standing UV filters (vide infra). Secondary maxima are the result of Fabry−Perot oscillations resulting from the interference between beams reflected at the upper and bottom face of the multilayer.

Fitting of the reflectance spectra is performed employing a model based on the scalar wave approximation and allows us to estimate the refractive index of each layer,[15,25] which can be related to porosity using the well-known Bruggeman equation. Using a code written in MATLab that finds the optimum fitting, we estimate the porosity in TiO_2 and SiO_2 layers as 49 and 39%, respectively. After the multilayer is infiltrated with PDMS ($n = 1.43$) and cured in a stove, the peak shifts to lower energies indicating that the average refractive index increases due to the replacing of air into the pores by PDMS. It can be seen how the dielectric contrast is barely affected, as the almost invariable peak width and intensity measured from the infiltrated lattice indicates. To avoid optical interferences caused by the PDMS layer accumulated on top, this is removed mechanically at room temperature without any previous treatment with liquid nitrogen (see Experimental Section). In Figure 4, we show the reflectance obtained before (thick solid line) and after (thin solid line) infiltrating a 10 layer 1DPC, along with their

(23) Calvo, M. E.; Sánchez-Sobrado, O.; Colodrero, S.; Míguez, H. *Langmuir* **2009**, *25*, 2443.
(24) Sozuer, H. S.; Haus, J. W.; Inguva, R. *Phys. Rev. B* **1992**, *45*, 13962.
(25) Fuertes, M. C.; López-Alcaraz, F. J.; Marchi, M. C.; Troiani, H. E.; Míguez, H.; Soler Illia, G.J.A.A *Adv. Funct. Mater.* **2007**, *17*, 1247.

respective fitting spectra (thick and thin dashed lines, correspondingly). Calculated porosities after infiltration are 40 and 2% in TiO_2 and SiO_2 layers, respectively. The larger polymer fraction load in SiO_2 layers versus TiO_2 ones might be explained in terms of the surface affinity between the pore walls and the PDMS. Theoretical calculations predict a strong interaction between PDMS and SiO_2 particles.[26]

The high flexibility of PDMS is conferred to the host multilayer, which causes that the hybrid ensemble can be easily lifted-off entirely from the substrate. Nevertheless, if this process is carried out at room temperature (reproducing the standard practice followed in soft lithography to replicate surface patterns[19]) only the accumulated PDMS on top of the multilayer is removed, the 1DPC filled with polymer remaining adhered to the substrate. This is a consequence of the viscoelastic properties of PDMS at room temperature. Stretching forces acting during the lifting-off causes the elongation of the polymer chains until rupture of such branches right at the interface between the top layer of the Bragg mirror and the overlayer. Connectivity to infiltrated layers is done across the pores of the SiO_2 layer. As the T_g temperature of PDMS is approximately 150 K,[18] it is necessary to go below this temperature to induce a phase transition that diminishes the elasticity of the PDMS. Best results were obtained when samples were immersed in liquid nitrogen (77 K). Once removed and heated to room temperature, self-standing samples present high flexibility, bright colors at photonic band gap frequencies, and transparency at spectral regions out of the expected forbidden band. Pictures illustrating these features are displayed in Figure 5. Optical interference filters prepared with different lattice parameter to select the reflectance peak over the entire visible spectrum are presented in Figure 5a. In Figure 5b, we show the optical response of a flexible filter. The green color reflected from the sample surface arises from the position of the Bragg peak at 540 nm and the red color reflected in the silicon wafer placed in the back corresponds to the light transmitted through the pass band of the filter. The flexibility of these photonic crystals is illustrated by the picture shown in images c and d in Figure 5. Finally, Figure 5e is a photograph of a red flexible multilayer peeled and taken off using a pair of tweezers. In this image we also show the substrate where the multilayer was deposited and infiltrated. The edges of the multilayer were not removed in order to demonstrate that the infiltrated PDMS permits us to completely and cleanly cut and lift the stack, thus confirming that the polymer infiltration is effective and continuous across the entire multilayer, which in this case is approximately 1100 nm wide. These images also point to the possibility to obtain flexible filters in a variety of shapes and thickness.

Design of Flexible and Adhesive Ultraviolet Interference Filters. One of the most important applications in protective coatings is the shielding of UV solar radiation to avoid undesirable photochemical reactions or due to the probed carcinogenic action of these rays over the skin.[27] The harmful wavelength range includes the less energetic and well-known UVA radiation ($320 < \lambda < 400$ nm).[28] Current technology for UV shielding is based on the inclusion of a series of compounds that absorb photons in the UV region into a matrix, which may be liquid or solid.[29] Protection is achieved by the interaction of the photons with the electronic levels of the absorber species. This mechanism implies in most cases the production of an electron−hole pair, both of them very reactive chemical species that can lead to toxic degradation products or potentially dangerous chemicals.[30] In this aspect, the use of interference filters as UV protection coatings could be advantageous with respect to absorption filters because the mechanism of shielding is based on the reflection of the incident photons, with no generation of reactive species and no heat accumulated or dissipated, which prevents any secondary undesirable chemical reactions.

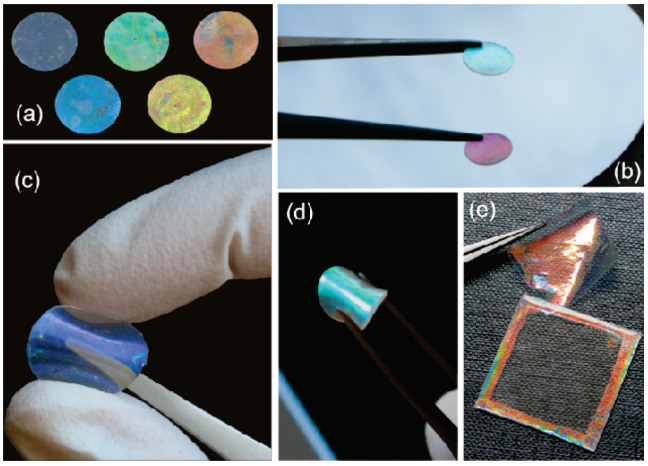

Figure 5. Photographs of some flexible interference filters: (a) a 12-layer 1DPC of different lattice parameters cut in circles; (b) an example of the colors obtained by reflection and transmission of a self-standing 1DPC; (c) a flexible and transparent violet self-standing 1DPC; (d) another example of flexibility and color; (e) flexible red mirror lifted from the substrate to which it was deposited (also shown).

The preparation method herein described allows for obtaining mirrors with a Bragg peak in the UV region, and hence they are suitable candidates to be used as flexible interference filters to protect against UV radiation. The possibility to protect human skin is supported by the biocompatibility of all compounds involved, as well as to the ability to control adhesion our method provides. One must keep in mind that the TiO_2 nanoparticles present in the multilayer already absorb light efficiently below 340 nm, which coincides with the so-called UVB range. To achieve and extend protection against the incident UVA rays ($320 < \lambda < 400$ nm), it is necessary to overlap the photonic band gap of the

(26) Tsige, M.; Soddemann, T.; Rempe, S. B.; Grest, G. S.; Kress, J. D.; Robbins, M. O.; Sides, S. W.; Stevens, M. J.; Webb, E. *J. Chem. Phys.* **2003**, *118*, 5132.
(27) Pearlman, D. A.; Holbrook, S. R.; Pirkle, D. H.; Kim, S. H. *Science* **1985**, *227*, 1304.
(28) Armstrong, B. K.; Kricker, A. *J. Photochem. Photobiol., B* **2001**, *63*, 8.
(29) Cole, C. A.; Vollhardt, J.; Mendrok, C. *Clinical Guide to Sunscreens and Photoprotection*; Lim, H. W., Draelos, Z. D., Eds.; Informa Healthcare: New York, 2009; pp 39−51.
(30) Bolton, K.; Martincigh, B. S.; Salter, L. F. *J. Photochem. Photobiol.* **1992**, *63*, 241.

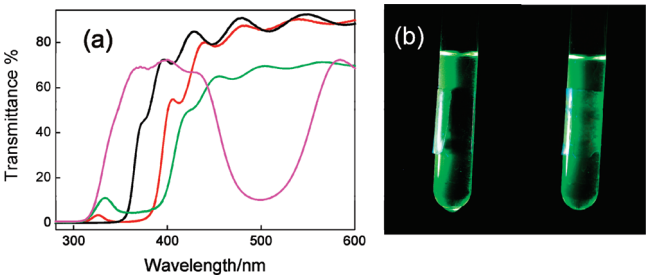

Figure 6. (a) Transmittance spectra of the interference filter at various preparation stages. 1DPC deposited on glass, air-filled (black line), and PDMS-infiltrated (red line); self-standing 1DPC (green line). (b) Photographs taken from the back side of two test tubes containing a dye solution excited under UV light. The tube on the left is covered with a 1DPC that protects in UV region (green spectrum in panel a), whereas the tube on the right is covered with a 1DPC that protects in a visible region (magenta spectrum in panel a).

multilayer with the electronic band gap. Additionally, it is necessary to obtain planar response in the transmittance Bragg peak to prevent the transmission of photons up to as close as possible to $\lambda = 400$ nm. These two requirements can be satisfied using dilute solutions of nanocolloids ($[SiO_2] = [TiO_2] = 2\%$), high final spin coating velocities ($v > 7000$ rpm), and an elevated number of stacked layers (>20). Starting SiO_2/TiO_2 multilayers, which will later host the PDMS compound, must be prepared with Bragg peaks centered around 350 nm, because PDMS infiltration will shift the peak central position to higher wavelengths (see Figure 4). Transmittance spectra of these samples are represented in Figure 6a. Stacked layers prepared in this way present a spectrum with only one apparent band (black line curve), which results from the overlap between the photonic and the electronic band gaps. Once the 1DPC is filled with polymer the Bragg peak shifts to lower energies and band observed is wider (red line curve). This implies that the sample is now able to shield simultaneously UVA and UVB ranges. When we remove the flexible multilayer from the substrate, spectrum bands position is not modified appreciably but intensities are affected because samples present a slightly higher diffuse scattering (green line curve). If protection from radiation within a larger spectral width is desired, two 1DPC with different lattice parameters can be stacked one after another.

A proof of concept of their potential use as flexible and adhesive UV protection coatings was attained by sticking two different 1DPC to the curved surface of two essay tubes containing an ethanolic solution of a luminescent compound, 3-hydroxyflavone. This dye absorbs photons in the UVA region of the spectrum and emits light at 530 nm. To increase the adherence of the flexible samples, we polymerize PDMS using a low elastomer precursor/curing agent ratio. One of the flexible 1DPCs used presented a reflectance spectrum like the one drawn with a green line in Figure 6a, this capable of blocking UVA light. The other one was used a blank test and consisted of a flexible 1DPC with the same number of layers that the previous case but with presented a reflectance peak near 500 nm (magenta spectrum in Figure 6a). Illumination with a UV lamp that presents its maximum intensity at $\lambda = 365$ nm reveals absence of luminescence within the

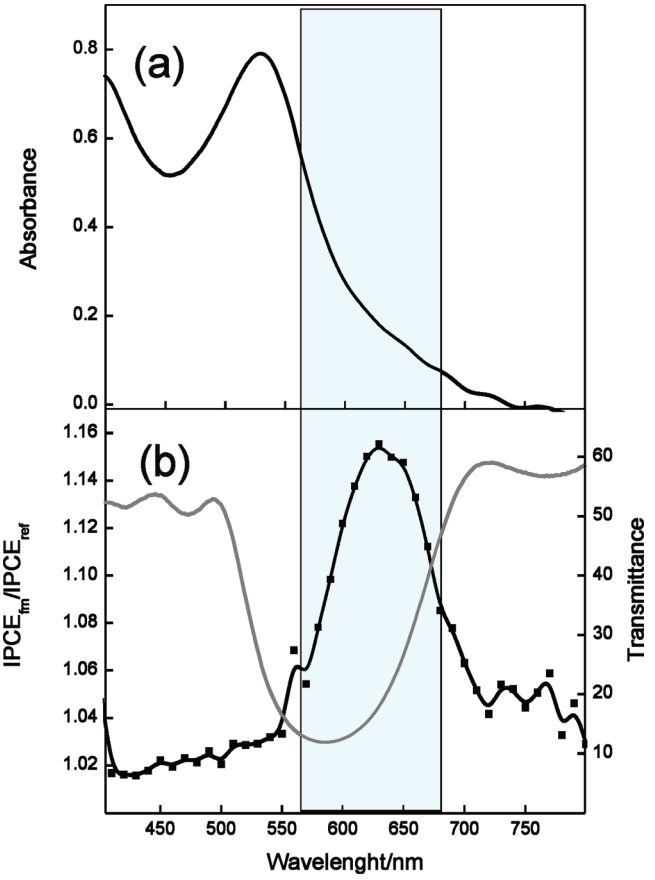

Figure 7. (a) Absorbance of a TiO_2 electrode sensitized with ruthenium bipyridyl dye. (b) IPCE ratio enhancement (squares line connected) obtained from a flexible Bragg mirror adhered at the external face of a DSSC counter electrode. Transmittance spectrum is represented in the gray line. The blue box is a guide to indicate the region of the spectrum where enhancement in IPCE is expected.

volume of the dye solution protected by the 1DPC (Left tube in Figure 6b). The border with the unprotected region can be readily distinguished. Contrarily, isotropic luminescence arising from the dye solution is observed for the case of the adhered 1DPC that presented the reflectance peak in the green, showing that in this case the UV light used to excite the dye could go through the PDMS and nanoparticle layers present in the blank sample.

Applications as Low-Weight, Frequency-Selective Mirrors. The characteristics of these self-standing 1DPC make them suitable to be integrated easily in devices that could benefit from the control of reflection and transmission of light at selected frequencies they offer. A straightforward application that illustrates this concept is the conformal attachment of our flexible and adhesive 1DPC to the rear external surface of the counterelectrode of a DSSC in order to reflect back into the device the non absorbed photons that have passed through the system. Briefly, DSSC are well studied photodevices that supports light to electric conversion and consists in a porous, electrically connected nanocrystalline TiO_2 (nc-TiO_2) film, which is coated by a monolayer of light-absorbing dye molecules.[31] The pores of the nc-TiO_2 film are filled with a liquid electrolyte (typically an I^-_3/I^-

(31) Grätzel, M. *Inorg. Chem.* **2005**, *44*, 6841.

redox couple). Incident photons pass trough the cell, where they are absorbed by the dye, usually a ruthenium complex. Photons that are not absorbed leave the cell and are lost as source of electric energy. In Figure 7a we show the absorbance ($\log(1/T)$) spectrum of a TiO_2 electrode deposited onto conductive glass and sensitized with ruthenium bipyridyl dye. It can be clearly seen that the light-harvesting efficiency of the dye diminishes toward the red part of the spectrum. Absorption at that range can be enhanced by placing a passive reflecting optical device behind, like our flexible 1DPC, which can be put into conformal contact with the external surface of the counterlectrode and possess a very low weight. Appropriate choice of the structural parameters of the 1DPC must be done to target the wavelength range at which absorbance is smaller. In Figure 7b, we present the enhancement produced in the efficiency of photon to electron conversion (IPCE, incident photon to current efficiency) by placing a flexible mirror that efficiently reflects red wavelengths on the back side of a DSSC (see square scatter graph). Such enhancement is calculated as the ratio between the IPCE of a DSSC to which a 1DPC has been attached and that of a reference consisting in the same DSSC without the adhesive mirror. The transmittance spectrum of the flexible mirror is included (solid lines). We can observe that the enhancement presents a similar dependence with wavelength than the reflectance of the mirror used.

Conclusions

We have introduced a method to build self-standing, flexible, adhesive, and biocompatible optical interference filters through infiltration and polymerization of an elastomer (polydimethylsiloxane) in a porous Bragg mirror prepared by alternating deposition of layers of TiO_2 and SiO_2 nanoparticles. By treating the infiltrated multilayer at temperatures below the glass transition of the polymer, it is possible to obtain a multifunctional material that combines the optical properties of the periodic nanoporous multilayer and the structural and physic-chemical characteristics of polydimethylsiloxane. Experimental demonstrations of their potential use as flexible and adhesive UV protecting filters, as well as of light highly efficient conformal back reflectors to enhance the efficiency of photovoltaic devices have been provided. We foresee very interesting applications of these PDMS-nanoparticle-based Bragg mirrors as transparent UV protectors of certain environments or, provided the required clinical tests have been realized, localized regions of the body.

Acknowledgment. We thank the Spanish Ministry of Science and Innovation for funding provided under Grants MAT2008-02166 and CONSOLIDER HOPE CSD2007-00007, as well as Junta de Andalucía for Grants FQM3579 and FQM 5247. M.E.C. thanks the Spanish Research Council for funding of his contract under the JAE program and Junta de Andalucia. The methods and materials herein presented are protected under Patent ES P200900275.

Supporting Information Available: Additional figure (PDF). This material is available free of charge via the Internet at http://pubs.acs.org.